

Planning of Hepatectomy for Tumor Resection: Resection Surface Construction and Optimization*

Wenyu Chen¹, Jiayin Zhou¹, Wei Xiong¹, Weimin Huang¹, Thiha Oo¹ and Sudhakar Kundapur Venkatesh²

Abstract—An interactive liver surgery planning system has been developed to construct and optimize the resection plan. With this system, the segmentation results of the liver and its components (such as tumors and vessels) are comprehensively visualized for surgeons to have an intuitive understanding of the internal anatomical structure of the liver. This system will also allow surgeons to interactively create and modify a resection plan on the virtual liver model. The resection surface, whose boundary is a closed curve, will be automatically constructed with the safe resection margins of tumors. Different from other systems, our developed system is able to generate the safety margins to all tumors. During surgery, a larger resection surface may cause potentially more bleeding and other complications. Therefore, area minimization is applied during the resection surface construction by adopting the minimal area mesh, which is a smooth surface with minimal area. After these virtual modifications, the resultant resection surface indicates the route to cut the liver for tumor removal. The volumes for both resected liver and residual liver are calculated for clinical decision making.

I. INTRODUCTION

Surgical resection is an important method for the treatment of liver tumor. As the interior structure of a human liver is complex and varies from patient to patient, surgeons need to understand the anatomic structure of the liver and its components by figuring out the relationships between the hepatic vein, the portal vein and tumors for a specific patient before a liver surgery. A preoperative planning system would help surgeons to make decisions on whether or not to perform a surgery, as well as how to perform it. Traditional surgery planning is usually based on visual observation of a series of two-dimensional (2D) computed tomography (CT) images. It is difficult to visualize a complex three dimensional anatomy with 2D images. A computer-aided liver surgery planning system can help in segmenting the liver, vessels and tumors in the CT images, providing intuitive visualization of the liver components and planning a proper resection route for the operation.

Resection of a tumor with safety margins that includes normal appearing liver parenchyma helps in removal of entire tumor as well as the adjacent area with microscopic tumor extension so as to reduce local recurrence. Two methods have been adopted to guarantee the safety margins

in different preoperative planning systems: local editing and global interpolation. In a local editing solution, a resection surface is first initialized as a grid mesh defined by the grid points on a plane, then interactively modified by grid points repositioning. Once a grid point is modified, the surgeon needs to input a deformation radius and a height. The grid mesh is deformed by automatically updating the nearby grid points using a cosine function to control the movement. The modification is restricted within a local region controlled by the deformation radius. Users need to repeatedly modify the resection surface until all safety margins are satisfied. Refinement may be required to make the surface smooth by adding more grid points. Such solutions are adopted by some commercialized systems such as MeVisLab [1], Mint Liver [2], Scout Liver [3], and Myrian XP Liver [4]. The global interpolation solutions obtain a resection surface as an interpolation to a set of markers, which can be either on the liver boundary or inside the liver. Making the interior markers to satisfy the safety margins may not guarantee the safety margins for the interpolated resection surface. Thus, if a safety margin is not satisfied, the surgeon is required to repeatedly modify the interior markers or insert more interior markers. Compared with the local editing solutions, the global interpolation solutions are better in smoothness. MITK [5] adopts a thin plate spline interpolation to obtain the resection surface [6].

In the aforementioned commercial planners, the creation and modification of the resection surfaces highly depend on user interactions. Multiple interactions will be required if the surgeon wants to maintain a good tumor safety margin. Precise liver surgery has been proposed and widely studied in recent years [7]. The target is to balance safety and effectiveness. For the resection surface construction, guaranteeing safety margin is an important criterion. However, other factors need to be taken into account as well during the planning. For example, the residual volume should be maximized and the potential bleeding should be minimized, which lead to an optimization problem. Several factors had been considered to evaluate different resection surfaces [8], which however have not yet been used in the construction of optimized surfaces. The difficulty is that it is a non-linear optimization problem. As a matter of fact, existing planners have not provided such a tool to assist the surgeon during the planning.

The present paper describes a preoperative planning system, which provides a simple yet flexible user interface for the surgeon to interact with the liver models. Surgeons only need to input required safety margins for different tumors

* This work is supported by a research grant (JCOAG03-FG05_2009) from the Joint Council Office, Agency for Science, Technology and Research (A*STAR), Singapore.

¹ Wenyu Chen, Jiayin Zhou, Wei Xiong, Weimin Huang and Thiha Oo are with Institute for Infocomm Research, Agency for Science, Technology and Research, Singapore

² Sudhakar Kundapur Venkatesh is with Mayo Clinic in Rochester, Minnesota, USA

and interactively edit a few control points on the boundary of the surgery plan. By solving a constrained optimization problem, our system automatically provides a minimum-area resection surface with safety margins guaranteed.

II. METHODOLOGY AND PROCEDURE

Fig.1 shows the flowchart of our planning system. Using the segmentation results from our previous work [9], comprehensive visualization renders liver components separately by adopting blending, 3D texture and so on (Fig.2). The resection surface will cut the liver into two parts: resected lobe and residual lobe. The volume for each lobe will be calculated and presented. The resection surface is controlled by its boundary. The users can interactively adjust the resection plan by editing the boundary and changing the safety margins (Fig.4). Our algorithm will automatically update the resection surface guaranteeing safety margins.

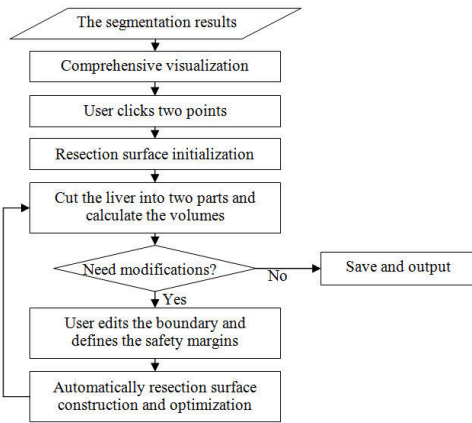


Fig. 1. The flowchart of the planning system.

A. Comprehensive visualization

In current clinical practice, the primary methods of liver analyses depend on the clinicians to visually inspect the CT images. This requires much expertise in discriminating vessels, tumors and the liver. Comprehensive visualization presents the liver data in a more accessible/intuitive manner to reduce the workload. Clinicians are able to check different liver components and choose to visualize any combination of the liver components. This would help them not only understand the relationship between the tumor and the vessels, but also see how different parts of the liver are affected by the resection. The surgeon can check which portions of the hepatic vein and the portal vein are removed in the planned resection (Fig.2(a)), and what are the surrounding organs following a predefined resection surface (Fig.2(b)).

B. Resection surface initialization

Clinicians are familiar with 2D operations as they usually work on 2D CT images. The initialization is implemented in a 2D manner. Users can rotate the scene to any angle and draw a line by clicking two points on the screen. A 3D plane perpendicular to the screen interpolating the two points is initialized as a resection surface (Fig.3).

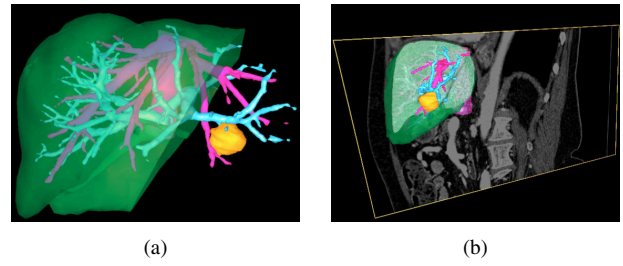


Fig. 2. Comprehensive visualization: (a) blending; and (b) 3D texture.

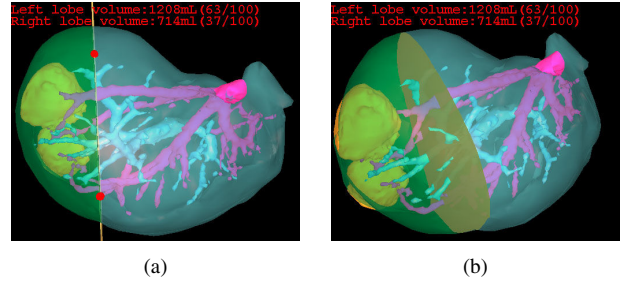


Fig. 3. Surface initialization and volume calculation: (a) the initial view; and (b) the rotation view.

C. Surface cutting and volume calculation

Once a cutting surface is defined, the system cuts the liver into resected lobe and residual lobe. The volumes of the resected and residual lobes will be provided by the system (Fig.3). If the residual liver volume is not enough to sustain life or may cause liver insufficiency, surgeons may not like to perform the surgery as planned or modify the surgery.

D. Interactive modification

Users can interactively adjust the surgery plan by editing only a few the control points on the boundary, or by adjusting the safety margins. Our system takes care of the interior portion of the resection surface to guarantee the safety margin to each tumor. Users are not required to input any interior marker (Fig.4).

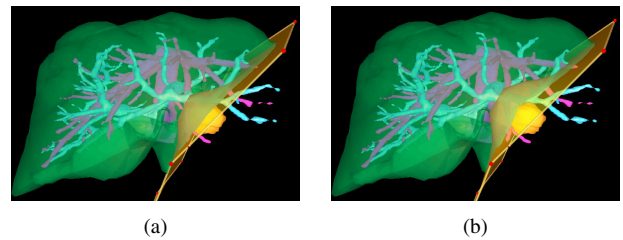


Fig. 4. Safety margin modification: (a) 5 mm; and (b) 10 mm.

E. Resection construction and optimization

The advantages of using our system lie in the functions of resection surface construction and optimization. Besides guaranteeing safety margins to different tumors, the system also optimizes the resection plan by minimizing the area of the resection surface. Fig.5 shows the flowchart of the optimization process. The part in dash box is one iteration. Before and after each iteration, the surface area changes

from S to S' . The algorithm will stop in finite iterations until the absolute area difference is smaller than a tolerance, i.e. $|S - S'| < \varepsilon$. The final resection surface is presented as a minimal area mesh.

A minimal area mesh can be constructed using the vertex-based algorithm, which minimizes the total area of the surface by minimizing the area around each vertex [10]. However, with such an algorithm, the triangles comprising the resection surface cannot guarantee the safety margin. Alternatively, during an iteration, a triangle-based algorithm is developed to update all interior triangles to guarantee the safety margin and minimize the resection area.

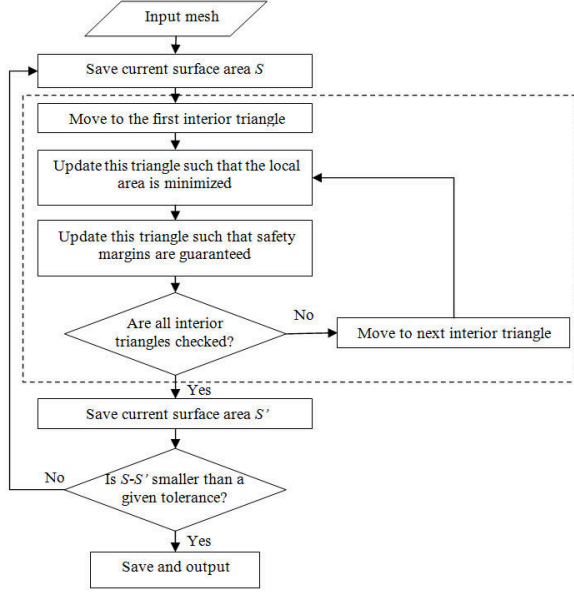


Fig. 5. The flowchart of resection surface construction and optimization.

1) *Area minimization*: For a triangle T with vertices $\mathbf{R}_0, \mathbf{R}_1, \mathbf{R}_2$, its 1-ring neighboring region Φ_T contains all the triangles that use \mathbf{R}_i as one vertex. In Fig.6, Φ_T is bounded by the polygon defined by vertices $Q_{i,j}$, which are the neighboring vertices of \mathbf{R}_i for $i = 0, 1, 2$. The triangle T should be updated such that the area of Φ_T is minimized. The problem can be formulated as

$$\min : S(\mathbf{R}_0, \mathbf{R}_1, \mathbf{R}_2) = \frac{1}{2} \sum_{i=0}^2 \sum_{s=0}^{n_i-1} \sqrt{(\mathbf{R}_i \mathbf{Q}_{i,s} \otimes \mathbf{Q}_{i,s} \mathbf{Q}_{i,s+1})^2} + \frac{1}{2} \sum_{i=0}^2 \sqrt{(\mathbf{R}_i \mathbf{R}_{i+1} \otimes \mathbf{R}_{i+1} \mathbf{Q}_{i+1,0})^2} + \frac{1}{2} \sqrt{(\mathbf{R}_0 \mathbf{R}_1 \otimes \mathbf{R}_0 \mathbf{R}_2)^2}.$$

Suppose $\frac{\partial F}{\partial \mathbf{R}_k} = \left(\frac{\partial F}{\partial (\mathbf{R}_k)_x}, \frac{\partial F}{\partial (\mathbf{R}_k)_y}, \frac{\partial F}{\partial (\mathbf{R}_k)_z} \right)^\perp$ (\perp is the transpose

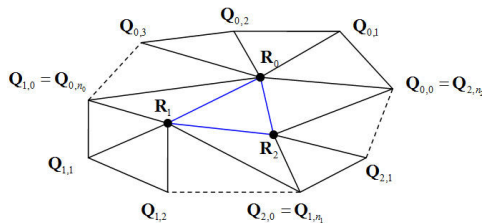


Fig. 6. The 1-ring neighboring region of a triangle.

operator). The partial differential of the target function gives

$$4 \frac{\partial S}{\partial \mathbf{R}_k} = 2 (\mathbf{D}_k^1 + \mathbf{E}_k^1 + \mathbf{F}_k^1) \mathbf{R}_k - 2 \mathbf{E}_k^1 \mathbf{R}_{k+1} - 2 \mathbf{F}_k^1 \mathbf{R}_{k-1} - 2 \left(\sum_{s=0}^{m_i-1} \mathbf{D}_{k,s}^1 \mathbf{Q}_{k,s} \right)^\perp,$$

where $\mathbf{D}_{k,s}^1, \mathbf{D}_k^1, \mathbf{E}_k^1, \mathbf{F}_k^1$ are 3×3 matrices as

$$\mathbf{D}_{k,s}^1 = \frac{|\mathbf{Q}_{k,s} \mathbf{Q}_{k,s+1}|^2 \begin{pmatrix} 1 & 0 & 0 \\ 0 & 1 & 0 \\ 0 & 0 & 1 \end{pmatrix} - (\mathbf{Q}_{k,s} \mathbf{Q}_{k,s+1})(\mathbf{Q}_{k,s} \mathbf{Q}_{k,s+1})^\perp}{\sqrt{(\mathbf{R}_k \mathbf{Q}_{k,s} \otimes \mathbf{Q}_{k,s} \mathbf{Q}_{k,s+1})^2}},$$

$$\mathbf{D}_k^1 = \sum_{s=0}^{n_k-1} \mathbf{D}_{k,s}^1,$$

$$\mathbf{E}_k^1 = \frac{|\mathbf{R}_{k+1} \mathbf{R}_{k+2}|^2 \begin{pmatrix} 1 & 0 & 0 \\ 0 & 1 & 0 \\ 0 & 0 & 1 \end{pmatrix} - (\mathbf{R}_{k+1} \mathbf{R}_{k+2})(\mathbf{R}_{k+1} \mathbf{R}_{k+2})^\perp}{\sqrt{(\mathbf{R}_k \mathbf{R}_{k+1} \otimes \mathbf{R}_{k+1} \mathbf{R}_{k+2})^2}},$$

$$+ \frac{|\mathbf{R}_{k+1} \mathbf{Q}_{k+1,0}|^2 \begin{pmatrix} 1 & 0 & 0 \\ 0 & 1 & 0 \\ 0 & 0 & 1 \end{pmatrix} - (\mathbf{R}_{k+1} \mathbf{Q}_{k+1,0})(\mathbf{R}_{k+1} \mathbf{Q}_{k+1,0})^\perp}{\sqrt{(\mathbf{R}_k \mathbf{R}_{k+1} \otimes \mathbf{R}_{k+1} \mathbf{Q}_{k+1,0})^2}},$$

$$\mathbf{F}_k^1 = \frac{|\mathbf{R}_{k-1} \mathbf{Q}_{k,0}|^2 \begin{pmatrix} 1 & 0 & 0 \\ 0 & 1 & 0 \\ 0 & 0 & 1 \end{pmatrix} - (\mathbf{R}_{k-1} \mathbf{Q}_{k,0})(\mathbf{R}_{k-1} \mathbf{Q}_{k,0})^\perp}{\sqrt{(\mathbf{R}_{k-1} \mathbf{R}_k \otimes \mathbf{R}_{k-1} \mathbf{Q}_{k,0})^2}}.$$

Setting the derivative to zero leads to a solution to the minimization problem. However, it is difficult to solve it directly as it is non-linear. A local mechanism can be adopted to iteratively approximate the solution. Suppose

$$\mathbf{R} = (\mathbf{R}_0, \mathbf{R}_1, \mathbf{R}_2)^\perp,$$

$$\mathbf{A}_1 = \begin{pmatrix} \mathbf{A}_0^1 \\ \mathbf{A}_1^1 \\ \mathbf{A}_2^1 \end{pmatrix} = \begin{pmatrix} \mathbf{D}_0^1 + \mathbf{E}_0^1 + \mathbf{F}_0^1 & -\mathbf{E}_0^1 & -\mathbf{F}_0^1 \\ -\mathbf{F}_1^1 & \mathbf{D}_1^1 + \mathbf{E}_1^1 + \mathbf{F}_1^1 & -\mathbf{E}_1^1 \\ -\mathbf{E}_2^1 & -\mathbf{F}_2^1 & \mathbf{D}_2^1 + \mathbf{E}_2^1 + \mathbf{F}_2^1 \end{pmatrix},$$

$$\mathbf{B}_1 = (\mathbf{B}_0^1, \mathbf{B}_1^1, \mathbf{B}_2^1) = \left(\sum_{s=0}^{m_0-1} \mathbf{D}_{0,s}^1 \mathbf{Q}_{0,s}, \sum_{s=0}^{m_1-1} \mathbf{D}_{1,s}^1 \mathbf{Q}_{1,s}, \sum_{s=0}^{m_2-1} \mathbf{D}_{2,s}^1 \mathbf{Q}_{2,s} \right)^\perp.$$

Then the solution becomes

$$\frac{\partial S}{\partial \mathbf{R}} = \frac{1}{2} \begin{pmatrix} \mathbf{A}_0^1 \mathbf{R} - \mathbf{B}_0^1 \\ \mathbf{A}_1^1 \mathbf{R} - \mathbf{B}_1^1 \\ \mathbf{A}_2^1 \mathbf{R} - \mathbf{B}_2^1 \end{pmatrix} = \frac{1}{2} (\mathbf{A}_1 \mathbf{R} - \mathbf{B}_1) = 0 \Rightarrow \mathbf{R} = (\mathbf{A}_1)^{-1} \mathbf{B}_1.$$

Since the right hand side of the equation also contains \mathbf{R}_i , the above equation cannot be considered to be an explicit solution for \mathbf{R}_i . However, it presents a way to update vertices $\mathbf{R}_i, i = 0, 1, 2$ iteratively by

$$\bar{\mathbf{R}} = (\mathbf{A}_1)^{-1} \mathbf{B}_1.$$

2) *Guaranteeing safety margin*: This is to update the triangle T so that Φ_T can keep the safety margins to different tumors in the following two steps:

Step 1: Move the triangle along its normal direction until the safety margins to tumors for this triangle are guaranteed.
Step 2: Move each vertex R_i along its normal direction until the safety margins for triangles $\Delta R_i Q_{i,j} Q_{i,j+1}$ are guaranteed.

In each iteration, the two operations appear to be incompatible. *Guaranteeing safety margin* does not minimize the surface area, while *area minimization* cannot guarantee the safety margin. However, after enough number of iterations, each operation only has a tiny change to the surface. The algorithm can provide a solution guaranteeing the safety margin and minimizing the area under a given tolerance.

III. EXPERIMENTAL RESULTS

Fig.7 is a case to resect a single tumor. The surgeon only need to modify the 7 control points (red points in Fig.7(a)) on the boundary of the resection surface. By default, the surface resects the tumor with a 10 mm safety margin (Fig.7(a,b)). With the same control points, updating safety margin to 20 mm will automatically create a new resection surface (Fig.7(c,d)). Since the tumor locates in the left lobe, the left lobe is resected and the volume of each lobe is listed in Table I. Our system can also handle multiple tumors. Fig.8 is another case where the right lobe containing two tumors is resected. In the third case (Fig.9), the tumor is close both to the middle hepatic vein and the right hepatic vein. As a result, the right lobe has to be resected. However, as shown in Table I, the residual volume is too small for the patient to survive thus this case is not surgically resectable.

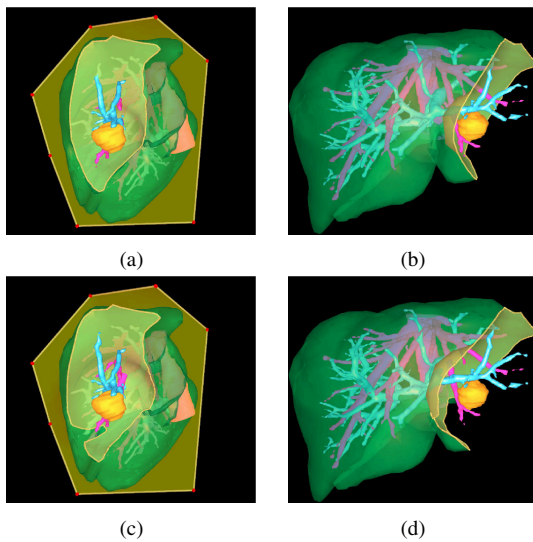


Fig. 7. Case 1: (a,b) 10 mm; and (c,d) 20 mm.

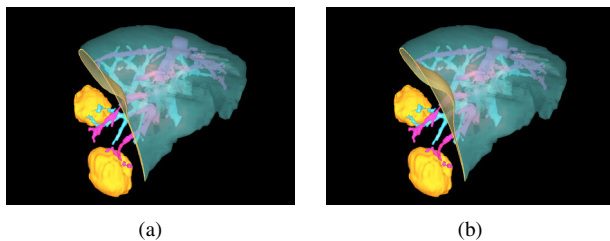


Fig. 8. Case 2: (a) 10 mm; and (b) 20 mm.

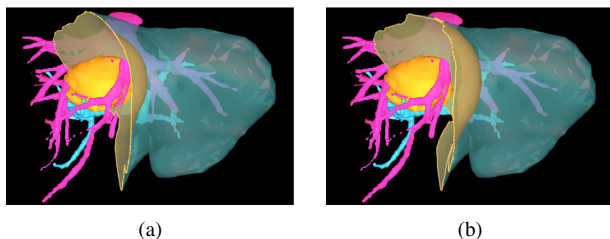


Fig. 9. Case 3: (a) 10 mm; and (b) 20 mm.

TABLE I
STATISTICS OF DIFFERENT CASES

Cases	Safety margins	Resected volume	Residual volume	Operationable
Case 1	10 mm	103 ml	1072 ml	Yes
	20 mm	136 ml	1039 ml	
Case 2	10 mm	533 ml	1390 ml	Yes
	20 mm	598 ml	1325 ml	
Case 3	10 mm	1260 ml	535 ml	No
	20 mm	1382 ml	413 ml	

IV. CONCLUSIONS

Interactive editing is important for surgeons to perform the liver resection planning. The novelty of the proposed method is the tight integration of boundary editing, safety margin guarantee, and surface area minimization. Surgeons would need to edit only a few control points on the boundary of the resection surface without placing any markers within the interior of the liver to execute the planned resection. The safety margin to each tumor will be automatically guaranteed. The construction procedure is fast with minimal user interaction requirement.

REFERENCES

- [1] O. Konrad-Verse, B. Preim, and A. Littmann, "Virtual resection with a deformable cutting plane," in *Proceedings of simulation und visualisierung*, 2004, pp. 203–214.
- [2] F. Pianka, M. Baumhauer, D. Stein, B. Radeleff, B. Schmied, H. Meinzer, and S. Müller, "Liver tissue sparing resection using a novel planning tool," *Langenbeck's Archives of Surgery*, vol. 396, no. 2, pp. 201–208, 2011.
- [3] B. DuBray Jr, R. Levy, P. Balachandran, K. Conzen, G. Upadhyya, C. Anderson, and W. Chapman, "Novel three-dimensional imaging technique improves the accuracy of hepatic volumetric assessment," *HPB: the official journal of the International Hepato Pancreato Biliary Association*, vol. 13, no. 9, pp. 670–674, 2011.
- [4] H. Petrowsky, S. Breitenstein, K. Slankamenac, D. Vetter, K. Lehmann, S. Heinrich, M. DeOliveira, W. Jochum, D. Weishaupt, T. Frauenfelder, et al., "Effects of pentoxifylline on liver regeneration: a double-blinded, randomized, controlled trial in 101 patients undergoing major liver resection," *Annals of surgery*, vol. 252, no. 5, p. 813, 2010.
- [5] I. Wolf, M. Vetter, I. Wegner, M. Nolden, T. Böttger, M. Hastenteufel, M. Schöbinger, T. Kunert, and H. Meinzer, "The medical imaging interaction toolkit (mitk): a toolkit facilitating the creation of interactive software by extending vtk and itk," in *SPIE Medical Imaging*, 2004, pp. 16–27.
- [6] D. Maleike, M. Nolden, H. Meinzer, and I. Wolf, "Interactive segmentation framework of the medical imaging interaction toolkit," *Computer methods and programs in biomedicine*, vol. 96, no. 1, pp. 72–83, 2009.
- [7] S. Fan, "Precise hepatectomy guided by the middle hepatic vein," *Hepatobiliary Pancreat Dis Int*, vol. 6, no. 4, pp. 430–434, 2007.
- [8] D. Demedts, A. Schenk, C. Hansen, and H. Peitgen, "Evaluation of Resection Proposals for Liver Surgery Planning," in *Proceedings of CURAC*, 2010, pp. 13–16.
- [9] J. Zhou, W. Xiong, F. Ding, W. Huang, T. Qi, Z. Wang, T. Oo, and S. Venkatesh, "Liver workbench: A tool suite for liver and liver tumor segmentation and modeling," *Advances in Bio-Imaging: From Physics to Signal Understanding Issues*, pp. 193–208, 2012.
- [10] W. Chen, Y. Cai, and J. Zheng, "Constructing triangular meshes of minimal area," *Computer-Aided Design and Applications*, vol. 5, no. 14, pp. 508–518, 2008.